Suhas D Kshirsagar, M M Deshmukh / International Journal of Engineering Research and Applications (IJERA) ISSN: 2248-9622 www.ijera.com
Vol. 3, Issue 2, March -April 2013, pp.1368-1380

Thermal Design & Performance Of Combined Vapour Compression-Ejector Refrigeration System Using R600a

Suhas D Kshirsagar*, M M Deshmukh**
*(M.tech student, Department of Mechanical Engineering, Govt. College of Engineering Amravati,)
** (Asst. Professor, Department of Mechanical Engineering, Govt. College of Engineering Amravati,)

ABSTRACT

Combined vapour compression-ejector refrigeration system is proposed which uses the waste heat of condesor of simple vapor compression system and this heat is utilized to drive the binary ejector refrigeration system. The cooling effect produced by this binary system can be considered as input to the cooling effect of basic vapour compression system. Thermal design of this combined vapour compression-ejector refrigeration system(VCR-VER) is based on energy and mass conservation in each component.

The system performance is first analyzed for the on design conditions. The results show that the COP is improved by 3.086% for the proposed system. The system is then analyzed for variation of four important variables. MATLAB Simulink software is used to model the combined VCR-VER system. The system analysis shows that this refrigeration system can effectively improve the COP by the ejector cycle with the refrigerant which has high compressor discharge temperature.

Keywords – Combined VCR-VER system, ejector refrigeration, thermal design, performance

NOMENCLATURE

A	*area* (m^2)
h	*enthalpy (kJ /kg)*
m	*mass flow rate (kg /s)*
P	*pressure (Pa)*
Q	*heat load (kW)*
R	*radius (m)*
S	*Entropy (KJ/Kg.K)*
T	*temperature (K)*
V	*velocity (m /s)*
W	*work (kW)*
α_{PP}	*pressure ratio,* P_{13}/P_8
α_{PS}	*pressure lift ratio,* P_8/P_7
α_A	*area ratio,* A_m/A_t
η	*efficiency*
$\Phi_{ej,m}$	*coefficient accounting for friction loss during the mixing process*
ρ	*density* (kg/m^3)
γ	*gas specific heat ratio*
ω	*entrainment ratio,* m_7/m_{13}
ED	*Exergy destruction*

Subscripts

comp	*compressor*
cond,a	*condenser A*
cond,b	*condenser B*
B	*booster*
E	*evaporator*
ej	*ejector*
g	*generator*
m	*ejector mixing chamber*
p	*pump*
is	*isentropic process*
sat	*saturation state*
t	*ejector nozzle throat*
o	*reference state*
r	*reversible process*
1	*state of refrigerant at inlet to the compressor*
2	*state of refrigerant at outlet of the compressor*
3	*state of refrigerant at outlet of the condenser A*
4	*state of refrigerant at outlet of expansion valve A*
5	*state of refrigerant at inlet to the evaporator*
6	*state of refrigerant at outlet of the evaporator*
7	*state of (primary fluid) refrigerant at inlet to the ejector or outlet of Booster*
8	*state of refrigerant at outlet of ejector*
9	*state of refrigerant at outlet of condenser B*
10	*state of refrigerant at inlet to expansion valve B*
11	*state of refrigerant at inlet to pump*
12	*state of refrigerant at outlet of pump or inlet to the vapour generator*
13	*state of refrigerant at outlet of vapour generator or inlet to ejector (secondary fluid)*

1. INTRODUCTION

Refrigeration and air-conditioning systems are widely used in air-handling and cooling applications. Improved system performance will reduce energy consumption as well as reduce CO_2 emissions. Decreases of the condensation temperature and increases of the evaporation temperature or the liquid condensate subcooling will improve the COP of the refrigeration system. These improvements are limited in practice since these

temperatures depend on the environmental temperature and operating conditions.

According to the second law of thermodynamics (Clausius statement), heat cannot be transferred from low temperature body to high temperature body without an aid of external agency. Thus, heat rejected at the condenser is equal to the sum of heat absorbed in the evaporator and compressor work equivalent heat. The refrigerant at the compressor outlet is usually quite warm (usually 80-110°C for R134a and R22 air-conditioning systems); thus, a large amount of energy must be rejected to the environment in the condenser. This waste heat energy can be utilized to increase the refrigeration system performance. An ejector cooling system driven by low-grade heat energy can effectively use the waste heat to improve the system COP. An ejector based cooling system offers several advantages, such as no moving parts in the ejector, efficient utilization of the waste heat and low cost

This paper describes a refrigeration system that combines a basic vapor compression refrigeration cycle with an ejector cooling cycle. The ejector cooling cycle is driven by the waste

heat from the condenser of the vapor compression refrigeration cycle. The ejector secondary flow is compressed first by means of a booster to ensure that the ejector works at the right conditions. The obtained cooling capacity from the ejector cycle is directly fed into the evaporator of the vapor compression refrigeration cycle. The entire refrigeration system performance is simulated to analyze the effects of the condensation temperature, the evaporation temperature, the pressure ratio, the pressure lift ratio and the ejector area ratio on the system performance. The results are compared with a basic refrigeration system.

1.1 Development In Combined VCR-VER System

In 1996 Sun et al. (1996)[1] developed a theoretical study of a combined cycle, using a ejector system and an absorption cycle. The working fluid was a H_2O-LiBr mixture. The result of this study showed an improvement of the COP of around 20-40% with respect to a conventional single effect absorption cycle. The system was designed for air conditioning applications with

COP values of between1 and 1.5. Despite the obvious improvements in efficiency, the required generator temperatures being between 180 and 240 ºC were too high to be handled by low grade energy sources. Also, the paper does not describe the practical operative disadvantages due to the nature of the system.

In 1997, Sun realized a theoretical study of a hybrid ejector-compression refrigeration system (Sun, 1997)[2]. The system utilized a different refrigerant for each subsystem; water and R134a were used as working fluids for the ejector refrigeration system and the mechanical refrigeration system respectively. Designed for air conditioning applications, it used low grade energy sources with 80 ºC generator temperatures. The authors considered solar energy as an energy source with no cost; this resulted in very high COP values between 4 and 6.8, as they only considered the electrical energy utilized and not the required thermal energy.

Also, they confirmed that the electrical energy requirements were reduced to half of that required regarding a conventional MCRS. The author proposed the use of the energy savings for the solar collector amortization. In 1998 Sun presented a comparative study of the effect of using different working pairs in a HJCRS system (Sun, 1998a, b).

Refrigerant R718, the CFC's R11, R12, R113, the HCFC's R21, R123, R142b, the HFC's R134a, R152a, the organic compound RC318 and the azeotrope R500 were the refrigerants evaluated. The study utilized the Keenan ejector model and the Thermo-physical properties of the refrigerants were obtained using equations of state. The use of recovery heat exchangers was evaluated, concluding that the superheating of the fluid to the ejector reduces the entrainment rate as a consequence of the specific volume decreasing reducing the overall performance. The best working fluid pair was R718 (water) and R21for the JCRS and the MCRS respectively reaching an overall COP of over 0.7. By 2001 Huang et al. designed and evaluated an air conditioning HJCRS hybrid system using R141b in both mechanical an jet compression subsystems. They showed an interesting system configuration, taking the thermal energy from the gases at the exit of the mechanical compressor. For the simulation and design, they used their own ejector model previously developed. The compressor behavior was predicted with an isentropic coefficient calculated for the particular case. The study concluded that the COP improvement was around 18% with respect to a simple JCRS.

In 2004 Arbel and Sokolov (2004)[3] presented a theoretical study of a solar driven COMBINED VCR-VER using R142b as working fluid. The study compared the performance of the system with previous studies developed by Sokolov, where R113 was used. They showed not only technical but also ecological improvements by using R142b. At this time the use of R113 is prohibited.

The same year, Herna´ndez et al. (2004)[4] presented a theoretical study comparing the performance of R134a to R142b in a JCRS-MCRS cycle. The operating temperatures were selected considering an ice production application, driven by solar energy. The used the model developed by Lu to predict the behavior of ejector and the other devices were estimated by theoretical efficiencies. From this and previous studies an experimental

testing system for JCRS was developed which is installed at the refrigeration and heat pumps laboratory at the Centro de Investigacio´n en Energı´a de la UNAM in Temixco, Morelos, Me´xico and shown in Fig. 5. At the present time experimental measurements are almost ready to begin.

In 2005 Jaya et al. (2005)[5] theoretically compared a JCRS-MCRS using R124, R134a and R32 for evaporating temperatures between 5 and 15 ºC. They concluded that R32 gives the best COP value. Nevertheless R32 has drawbacks such as high generator pressures and high circulation ratios. They proposed the R134a as the preferred working fluid for low heat source temperature applications.

In 2007 Elakdhar et al. realized a theoretical study of a COMBINED VCR-VER for domestic refrigeration (Elakdhar et al., 2007)[6]. A simulation of the cycle was developed in FORTRAN and the thermo-physical properties were taken from REFPROP V8.0. The behavior of the system with different working fluids (R123, R124, R141b, R290, R152a, R717, R600a and R134a) was simulated. They obtained the best results for R141b. The system did not have an intercooler; the exit of the ejector was connected to the entrance of the compressor.

They showed an inversely proportional relation between the COP and the decrement of the secondary evaporator temperature. However, as in other studies, some of the research developed should be renewed mainly because of the use of CFC's (chlorofluorocarbons) based refrigerants. After the development of the Kyoto protocol the use of environmental friendly refrigerants such as HCFC's (Hydro chlorofluorocarbons) and hydrocarbons has been promoted.

In 2010, Petrenko et al. (2011)[8] presented a theoretical study of a trigeneration system that consisted of a cogeneration subsystem and a hybrid cooling subsystem. The combined VCR-VER cooling system included a mechanical compression and a jet compression refrigeration subsystem, using R744 (CO2) and R600 (butane) as working fluids, respectively. For the simulation they used an improved one-dimensional model which was validated with experimental data for several working fluids. The mechanical vapor compression subsystem was modeled using an isentropic compressor efficiency of 0.67 working under subcritical conditions. The cooling system was developed for a capacity of 10 kW and reached a total COP of 1.4 when operating under design conditions. The working fluids used met current environmental selection criteria.

The same year Vidal (Vidal and Colle, 2010)[9] carried out the simulation and thermo-economic optimization of a COMBINED VCR-VER cooling system. The working fluid for the mechanical compression subsystem was R134a whilstR141bwas proposed for the jet compression subsystem. The system used flat solar collectors to harness solar energy as the main power supply, having a gas burner as an auxiliary source. The authors discussed the importance of the proper selection of system components to obtain adequate payback periods. They pointed out the limitations of the JCRS and suggested the use of combined VCR-VER systems. The optimized system proposed had a cooling capacity of 10.5 kW and a COP of 0.89 when the generator, condenser, intercooler and evaporator temperatures were 80 ºC, 34 ºC, 19 ºC and 8 ºC respectively. The optimized solar collector area was assumed to be 105 m^2 for a solar fraction of 82%. The system was designed for an air conditioning application.

In 2012, Yinhai Zhu, Peixue Jiang (2012)[10] carried out the simulation of combined VCR-VER cooling system. They utilized the waste heat of basic compression system. Thus generator receives heat from basic compression system, thus creates vapours required to drive the ejector of ejector cycle. They found that hybrid refrigeration system with the parallel ejector cycle significantly improves the COP when the compressor discharge temperature is larger than 100 ºC. Simulations give an average COP increase for the hybrid system with R152a of 5.5% relative to the basic system and 8.6% with R22. The average COP increase of R134a system is about 0.7% due to its compressor discharge temperature is in the range of 70-90 ºC.

Table 4 summarizes the state of art for the COMBINED VCR-VER. It should be mentioned that other theoretical and experimental studies has been developed in the last years but they focused on the improvement of a specific system component, such as the ejector's geometry (Abdulateef et al., 2009[11]; Chunannond and Aphornratana, 2004[12]). However this work was focused on the improvements due to the use of different working fluids in simple and hybrid JCRS.

Table 1 Combined VCR-VER system from 1989 to 2007 [table taken from Gonza´lez Bravo et. al (2012)]

Author(year)	Refrigerant	Temperature[° C]	Cooling capacity(kW)	Total COP	Type of study
Sokolov and Hershgal (1989)	R114	T_{evap} = -8 T_{int} = NA T_{cond} = 30 T_{gen} = 86	2.9	0.4	Experimental
Da-Wen Sun et al. (1996)	LiBr-R717	T_{evap} = 10 T_{int} = NA T_{cond} = 22 T_{gen} = 210	NA	1.8	Theoretical
Da-Wen Sun (1997)	R718 and R134a	T_{evap} = 5 T_{int} = 25 T_{cond} = 35 T_{gen} = 80	5	5	Theoretical
Da-Wen Sun (1998 a,b)	R21 and R718	T_{evap} = 5 T_{int} = 30 T_{cond} = 40 T_{gen} = 70	NA	0.65	Theoretical
Huang et al. (2001)	R141b and R22	T_{evap} = 5 T_{int} = 25 T_{cond} = 40 T_{gen} = 70	5.2	2.5	Experimental
Arbel and Sokolov (2004)	R142b	T_{evap} = 4 T_{int} = 38 T_{cond} = 50 T_{gen} = 100	3.5	5	Theoretical
Herna´ndez et al. (2004)	R134a, R1142b	T_{evap} = -10 T_{int} = NA T_{cond} = 30 T_{gen} = 85	1	0.48	Theoretical
Jaya et al. (2005)	R124, R134a and R32	T_{evap} = -5 T_{int} = NA T_{cond} = 20 T_{gen} = 100	NA	0.7	Theoretical
Elakdhar et al. (2007)	R123, R124, R141b, R290, R152a, R717, R600a and R134a	T_{evap1} = 5 T_{evap2} = -30 T_{cond} = 42 T_{gen} = NA	NA	1.38	Theoretical
Petrenko et al. (2011)	R744, R600	T_{evap} = -20 T_{int} = 20 T_{cond} = 36 T_{gen} = 120	10	1.4	Theoretical
Vidal and Colle (2010)	R134a, R141b	T_{evap} = 8 T_{int} = 19 T_{cond} = 34 T_{gen} = 80	10.5	0.89	Theoretical
Yinhai Zhu, Peixue Jiang (2012)	R134a, R152a, R22	T_{evap} = -5 T_{int} =NA T_{cond} = 50 T_{gen} = 82.55	5.99	2.40	Theoretical

Note- T_{evap}, T_{cond},T_{gen}, T_{int} are the evaporation, condenser, generator and intercooler temperatures respectively.

2. System Description:

Fig. 1 shows the basic vapor compression refrigeration system. A compressor is used to drive the inverse Rankine cycle. The high temperature refrigerant at the compressor outlet rejects heat to the environment in the condenser. This waste heat energy can be utilized by an ejector cycle to

increase the refrigeration system COP. The refrigeration system in this study includes the basic refrigeration cycle and a heat driven ejector cooling cycle.

The ejector cooling cycle is connected in parallel with the basic refrigeration cycle as shown in The ejector cycle consists of an ejector, a condenser, a circulation pump, anexpansion device and a booster. The ejector is driven by high temperature vapor generated by the waste heat in the condenser of the basic cycle. The cooling capacity from the ejector cycle is injected into the basic cycle by means of two parallel expansion valves before the evaporator. The system functions can be briefly described as follows:

1. In the basic refrigeration cycle, high temperature vapor from the compressor rejects part of its sensible heat to the ejector cycle refrigerant in the generator. The condenser A is placed after the generator to make sure the refrigerant at the expansion valve inlet is all liquid. The evaporator in the basic refrigeration cycle provides the cooling.
2. In the ejector cooling cycle, the high temperature, high pressure refrigerant vapor (the primary flow) generated in the generator flows through the ejector and entrains the low temperature, low-pressure vapor (the secondary flow) from the evaporator outlet. The secondary flow from the evaporator is first compressed to a relatively high pressure in the booster and then enters the ejector. The primary and secondary flows mix in the ejector and then discharge to condenser B. After the condensation process, the refrigerant is divided into two parts, with one part pumped back to the generator and the other part flowing through expansion valve B and into the evaporator. The ejector cycle thus provides additional cooling capacity.

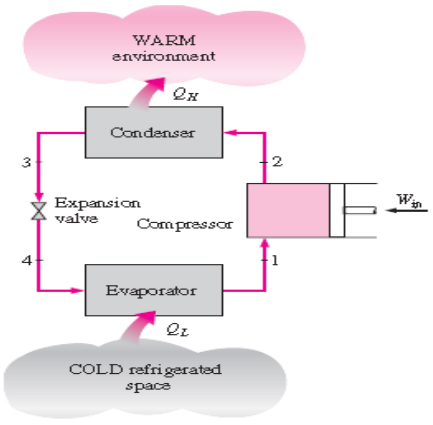

Figure 1 Vapour compression refrigeration system

3. Thermal Design And Simulation:

The refrigeration system is a combination of a basic compression refrigeration cycle and the ejector cycle. The governing equations are based on energy and mass balances for each component in the two cycles.

.

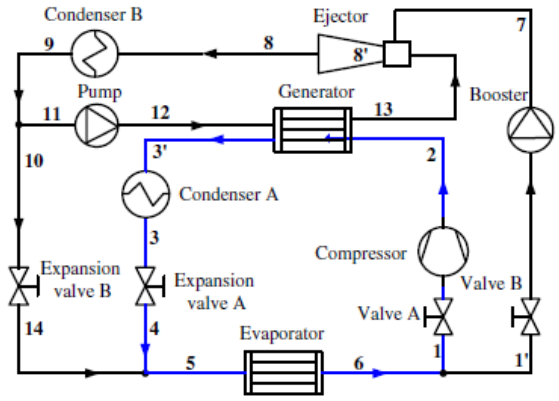

Figure 2 Combined VCR-VER system

3.1 Governing equations for the basic vapour compression cycle

3.1.1 Compressor

The compressor is assumed to be non-isentropic. Process 1-2s is an isentropic compression process, while process 1-2 is the actual compression process. The actual enthalpy of state 2 is expressed by:

$$h_2 = h_1 + (h_{2,s} - h_1) / \eta_c \quad (3.1)$$

Where, η_c is the isentropic efficiency of the compression process. The enthalpy and entropy of the refrigerant at state 1 are determined by the temperature and pressure at the compressor inle

$$h_1, s_1 = f(T_1, P_1) \quad (3.2)$$

The refrigerant enthalpy at state 2s for the isentropic process is:

$$h_{2,s} = f(s_{2,s}, P_2) \quad (3.3)$$

The power input to the compressor can be evaluated as:

$$W_c = m_1(h_2 - h_1) \quad (3.4)$$

3.1.2 Condenser/generator

In the combined VCR-VER system shown in Fig.2, low temperature fluid, which generates vapor by absorbing heat from the high temperature compressor discharge, becomes the working fluid to drive the ejector. Note that the condensing temperature in the basic refrigeration cycle is lower than the evaporating temperature of the ejector cycle. Therefore, only part of the sensible heat can be used to vaporizing the refrigerant of the ejector cycle in the generator. The total energy balance in the vapor generator is:

$$m_2(h_2 - h_{3'}) = m_{13}(h_{13} - h_{12}) \quad (3.5)$$

For the heat exchanger design, there is a minimum temperature difference at the generator's two sides:

$$T_2 \geq T_{13} + \Delta T_g ; T_{3'} \geq T_{12} + \Delta T_g \quad (3.6)$$

In addition, the evaporating process of the fluid in the generator is taking in constant temperature of T13. Therefore the used sensible heat of the

compressor discharge should satisfy the following equation:

$m_2(h_2 - h_{2x}) \geq m_{13}(h_{13,vapor} - h_{13,liquid})$ (3.7)

where,T2x =T13 + ΔTg , P2x = P2. The thermodynamic state of the fluid at the vapor generator exit (state 3') is then governed by the Eqn. (3.5) - (3.7), which are related to both the basic cycle and the ejector cycle. In this paper, the simulation is based on the minimum T2x in the generator. The fluid state at the generator exit is:

$T_{3'}, s_{3'} = f(P_{3'}, h_{3'})$. (3.8)

Assuming the refrigerant at the generator exit of the ejector cycle (state 13) is a saturated vapor:

$T_{13}, h_{13}, s_{13} = f_{sat}(P_{13})$ (3.9)

Where, P13 is the pump discharge pressure.

The heat load in the vapor generator is then:

$Q_g = m_1(h_2 - h_{3'})$ (3.10)

3.1.3 Condenser A

The conditions at state 3 for the condenser A shown in Fig. 1.3, assuming the refrigerant at the exit (state 3) is a saturated liquid, are:

$P_3, h_3, s_3 = f_{sat}(T_c)$ (3.11)

where, T_c is the condensing temperature. The outlet pressure is the compressor discharge pressure:

$P_3 = P_2$ (3.12)

The heat load for condenser A is then:

$Q_{CA} = m_2(h_{3'} - h_3)$ (3.13)

3.1.4 Evaporator

The function of the evaporator in the basic refrigeration system differs from that in the combined VCR-VER system. For the evaporator in Fig. 1.3, assume that the refrigerant at the exit (state 1) is super heated ΔT_e. The governing equations for the evaporator are then:

$P_1 = f_{sat}(T_e)$ (3.14)

$T_1 = T_e + \Delta T_e$ (3.15)

$h_1, s_1 = f(T_1, P_1)$ (3.16)

Where, T_e is the evaporating temperature. The cooling capacity of the basic refrigeration system is then:

$Q_e = m_1(h_3 - h_1)$ (3.17)

For the combined VCR-VER system in Fig. 2, the refrigerant after expansion valve B (state 14) and the refrigerant after expansion valve A (state 4) meet at the evaporator inlet (state 5).

The cooling capacity of the combined VCR-VER refrigeration system has two parts:

$Q_e = m_4(h_3 - h_1) + m_{14}(h_9 - h_1)$ (3.18)

Where, the cooling capacity of the ejector cycle, Q_{ej}, is:

$Q_{ej} = m_{14}(h_9 - h_1)$ (3.19)

A mass balance gives:

$m_4 + m_{14} = m_1 + m_7$ (3.20)

$m_1 = m_4$; $m_{14} = m_7$ (3.21)

The evaporator combines the basic vapor compression refrigeration cycle with the ejector cycle. The thermodynamic states of the fluid at states 7, 9 and 14 can be determined from the governing equations for the ejector cycle.

3.2 Governing equations for Ejector cycle :

3.2.1 Ejector

The ejector works as a compression device where the high pressure primary flow (state 13) entrains the low-pressure secondary flow (state 7) into the ejector. Previous studies have shown that the ejector performance is influenced by both the ejector geometry and the operating conditions. The ejector performance is usually evaluated based on the combined mass flow rates of the two flows. The mass flow rate of the primary flow of the ejector is determined by the ejector's structure and the thermodynamic properties of the primary flow. Assuming isentropic flow, the mass flow rate of the primary flow through the nozzle,m_{13}, when choked can be expressed by (Huang et al., 1999[12]; Zhu et al., 2007)[13]

$$m_{13} = A_t * \left(\psi_{ej,s}\, \gamma P_{13} \rho_{13}\right)^{\frac{1}{2}} * \left(\frac{2}{1+\gamma}\right)^{\frac{\gamma+1}{(2*(\gamma-1))}} \quad . \quad (3.26)$$

where $\psi_{ej,s}$ represents a coefficient related to the isentropic efficiency of the compressible flow in the nozzle and P_{13} and T_{13} are the pressure and temperature of the primary flow, respectively, at the ejector inlet.

The characteristics of the secondary flow in the ejector are more complex than those of the primary flow. In the critical mode, the secondary flow is choked in the ejector (hypothetical section 8') which determines the ejector performance. Zhu and Li (2009)[14] derived the following to calculate the secondary flow mass flow rate:

$$m_7 = \left(\frac{2\pi\rho_7}{R_m * R_{8'}}\right) * \sqrt{\left[\left(\frac{\gamma P_{8'}}{\rho_{8'}}\right) * \left\{\left(\frac{R_m^3}{6}\right) - ((R_m * R_{8'}^2)/2) + (R_{8'}^3/3)\right\}\right]} \quad . \quad (3.27)$$

Where$\rho_{8'}$, $P_{8'}$ and $V_{8'}$ are the density, pressure and velocity of the primary flow, respectively, at a hypothetical section where the secondary flow is choked and $R_{8'}$ is the radius of the mixing layer in this hypothetical section which can be expressed by

$$R_{8'} = \frac{R_t}{\emptyset_{ej,m}} * \left[\frac{[\![(2*\psi]\!]_{ej,s} * \left(\frac{P_{13}}{P_{8'}}\right)^{\left(\frac{\gamma-1}{\gamma}\right)} + 2 - 2*\psi_{ej,s}}{\gamma+1}\right]^{\frac{\gamma+1}{(4*(\gamma-1))}} * \left(\frac{\gamma-1}{[\![(2*\psi]\!]_{ej,s} * \left(\frac{P_{13}}{P_{8'}}\right)^{\left(\frac{\gamma-1}{\gamma}\right)} - 2*\psi_{ej,s}}\right)^{\frac{1}{4}} \quad . \quad (3.28)$$

The fluid properties of the primary flow at the hypothetical section 8' can be obtained based on the isentropic flow assumption:

$h_{13}, s_{13}, r_{13} = f(T_{13}, P_{13})$ (3.29)

$s_{8'} = s_{13}$ (3.30)

$x_{8'}, h_{8'}, r_{8'}, T_{8'} = f(s_{8'}, P_{8'})$ (3.31)

where, $x_{8'}$ represents the dryness fraction of the primary flow at the hypothetical section 8'.

The flow enthalpy at the ejector exit, h8, can be calculated from an energy balance for the primary flow and the secondary flow from the ejector inlet to the diffuser exit:

$h_8 = (m_{13}h_{13} + m_7h_7 - E_{loss}) / (m_{13} + m_7)$ (3.32)

where, E_{Loss} is the total kinetic energy loss for the primary flow and the secondary flow together in the ejector.

3.1.1 Condenser B

The refrigerant discharges heat in condenser B to the coolant.

Assuming the refrigerant at the exit (state 9) is saturated liquid, the governing equations for condenser B are:

$P_9, h_9, s_9 = f_{sat}(T_c)$ (3.33)

The heat load in condenser B is then:

$Q_{CB} = (m_7 + m_{13})(h_8 - h_9)$ (3.34)

3.1.2 Pump

The pump is a non-isentropic process. The actual enthalpy at the pump exit (state 12) can be expressed as:

$h_{12} = h_{11} + (h_{12,s} - h_{11}) / \eta_p$ (3.35)

where, η_p is the isentropic efficiency for the pumping process.

The thermodynamic states of fluid at state 11 are the same as those of fluid at state 9.

The enthalpy of the refrigerant at state 12s for an isentropic process is:

$h_{12,s} = f(s_{12,s}, P_{12})$ (3.36)

where, $s_{12,s} = s_{11}$

The power input to the pump can then be evaluated as:

$W_p = m_{12}(h_{12} - h_{11})$ (3.37)

3.1.3 Booster/ Low Pressure compressor

The pressure lift ratio between the back pressure and the suction pressure of the ejector in the combined VCR-VER refrigeration cycle, P_8/P_7, is much larger than that in the conventional ejector refrigeration cycle. For example, the pressure lift ratio is approximately 3.47 for R134awhen T_e = 0 ºC and T_c = 40 ºC. Note that the maximum pressure lift ratio of the ejector is limited by the working mechanism and is generally below 2.0. Therefore, a booster is used in the combined VCR-VER system to compress the vapor refrigerant before it enters the ejector. The booster can be a compressor designed to operate efficiently at a low compression ratio. The booster in the ejector cycle has two functions:

1. To ensure that the ejector works correctly. The ejector may not entrain the secondary flow and back flow may occur at a high-pressure lift ratio, P_8/P_7 (Huang et al., 1999[11]; Bartosiewicz et al., 2005).[16]

2. To increase the ejector performance. The ejector entrainmentratio increases with the suction pressure (Aphornratana et al., 2001[17]; Sun, 1997[18])

.

For a real non-isentropic vapor compression process, the actual enthalpy at the booster exit (state 7) can be expressed as:

$h_7 = h_{1'} + (h_{7,s} - h_{1'}) / \eta_b$ (3.38)

where, η_b is the isentropic efficiency of the compression process. The refrigerant enthalpy at state 7s for the isentropic process is:

$h_{7;s} = f(s_{7;s}, P_7)$ (3.39)

where, $s_{7,s} = s_{1'}$.

The power input to the booster is then:

$W_b = m_7(h_7 - h_{1'})$ (3.40)

3.2 Simulations Model:

Each component is designed with the help of equations described above in MATLAB Simulink software. The thermodynamic properties of refrigerant (i.e. R600a) have been taken from NIST library. In order to find out the performance, five variables has been chosen as described in Table 2

4. RESULTS AND DISCUSSION:

In the combined VCR-VER refrigeration system, the ejector working state significantly affects the whole system performance. The ejector cycle performance can be evaluated based on the entrainment ratio, ω, and the coefficient of performance, COP_{ej}:

$\omega = m_7 / m_{13}$ (4.1)

$COP_{ej} = Q_{ej} / Q_g + W_p + W_b$ (4.2)

The coefficient of performance of the combined VCR-VER refrigeration system, COP_2, is:

$COP_2 = Q_e / W_c + W_p + W_b$ (4.3)

For comparison, the coefficient of performance of the basic refrigeration system, COP_1, is:

$COP_1 = Q_e / W_c$ (4.4)

The present study used R600a (Isobutane) as the working fluids. Their thermodynamic properties were calculated based on the NIST library.

The combined VCR-VER refrigeration system has five independent design variables, the evaporating temperature, Te, the condensing temperature, Tc, the area ratio between the nozzle throat and the mixing chamber, α_A, the ratio of the ejector primary flow pressure to the ejector back pressure, α_{pp} and the pressure lift ratio of the ejector back pressure and the secondary flow α_{PS}. Te and Tc depend on the cooling load and the environmental temperature.

This study used -10 < Te <10ºC and 45 < Tc < 55ºC. On-design values for the five variables in the simulations are listed in Table 2.

Table 2.On design parameter

Variable	Value
T_e	-5ºC
T_c	50ºC
R_t	1.1045 mm
α_A	7.0
α_{pp}	2.1
α_{PS}	1.5

4.1 ON DESIGN PERFORMANCE

The simulation model is developed in MATLAB simulink model & the simulation results are listed in Table 3. Result shows that COP of R600a Combined VCR-VER system is 4.6% higher than its basic system.

One key advantage of the combined VCR-VER system is that the refrigerant after the expansion in the ejector cycle is directly fed into the coolant at the evaporator inlet. Thus, no heat exchanger such as a subcooler is needed and the irreversible losses in the heat exchanger are eliminated.

The off-design simulations used various T_e, T_c, α_A, α_{PP} and α_{PS}. Results were obtained by changing one variable while the others were fixed at their design point values. In each case, the ejector nozzle radius Rt is changed to control the mass flow rate m13, which is determined by the heat balance in the generator.

4.2 Effect of T_e

4.2.1 Effect of T_e on cooling capacity of combined VCR-VER system

Fig. 3 shows the effect of Te on the cooling capacity of the basic system and the combined VCR-VER system with R600a refrigerant for T_c = 50ºC, α_A= 7.0, α_{ps} =1.5 and α_{pp} = 2.1. The cooling capacity increases as the evaporating temperature increases. The combined VCR-VER refrigeration system provides much more cooling capacity than the basic system for the same power input with an increase of 1.6% with R600a compared with the basic system at T_e of -5 ºC

.

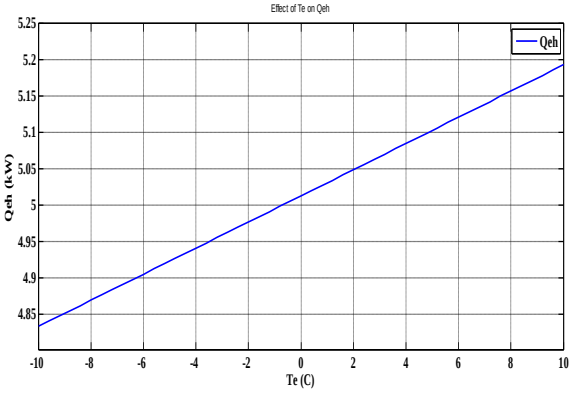

Fig. 3 Effect of T_e on cooling capacity, Q_{eh}

4.2.2 *Effect of T_e on entrainment ratio*

The variations of the entrainment ratio and ejector cycle COP with T_e are presented in Fig. 4. All the ejector entrainment ratio and ejector cycle COP is more or less constant with change in evaporator temperature. Although COP_{ej} is low compared to the compression refrigeration cycle COP, the ejector cycle improves the COP because the heat energy utilized in the ejector cycle is the waste heat from the compressor as shown in fig 5.

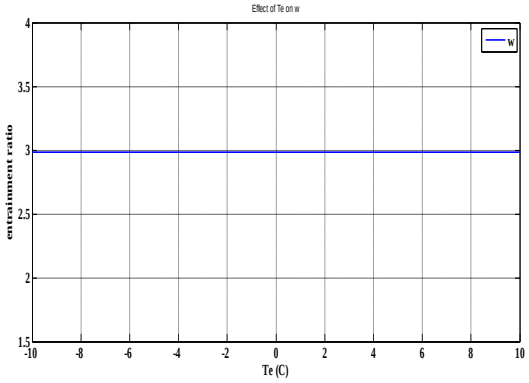

Fig.4 Effect of Te on entrainment ratio, ω

Table 3. On design performance of basic VCR and Combined VCR-VER system

Basic VCR system				**Combined VCR-VER system**							
$\dot{m}_1$ in Kg/s	Q_e in kW	W_{comp} in kW	COP_1	$\dot{m}_7$ in Kg/s	W_B in kW	W_P in kW	Q_{ej} in kW	Q_g in kW	COP_{ej}	COP_2	ΔCOP in %
0.01256	**4.665**	**12.1**	**0.3855**	**0.01256**	**0.2556**	**0.03505**	**0.2595**	**0.08249**	**0.6953**	**0.3974**	**3.086**

4.2.3 Effect of T_e on COP of combined VCR-VER system

Fig. 6 shows the effect of T_e on the COP of the combined VCR-VER systems and the COP improvement. The results show that the COPs of all systems increase with increasing evaporating temperature. The higher compressor discharge temperature results in more vapors generated in the generator

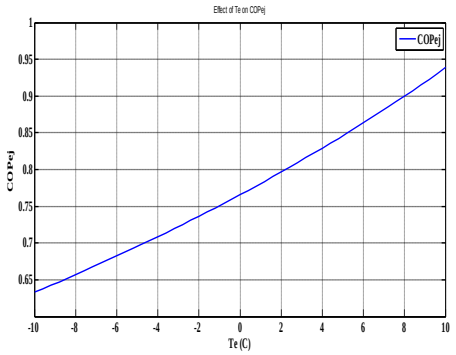

Fig 5 Effect on Te on COP of ejector cycle

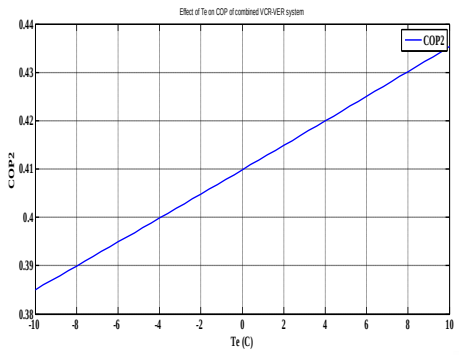

Fig 6 Effect on Te on COP of combined VCR-VER system, COP2

4.3 Effect of T_c

4.3.1 Effect of T_c on cooling capacity of combined VCR-VER system

Figure 7 shows the effect of Tc on the cooling capacities of system with R600a. The cooling capacity of R600a systems decrease as the condensing temperature increases because the enthalpy of fluid at state 3 increases as the condensing pressure increases when the refrigerant at state 3 is assumed to be saturated liquid.

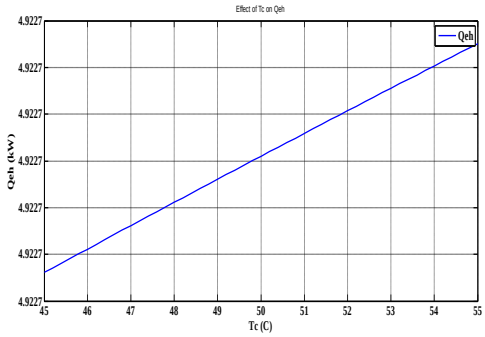

Fig 7 Effect of Tc on cooling capacity, Qeh

4.3.2 Effect of Tc on entrainment ratio

The variations of the entrainment ratio and ejector cycle COP with Tc are shown in Figure 8. The ejector entrainment ratio and ejector cycle COP decrease with T_c because the ejector condensing temperature equals to the condensing temperature T_c.

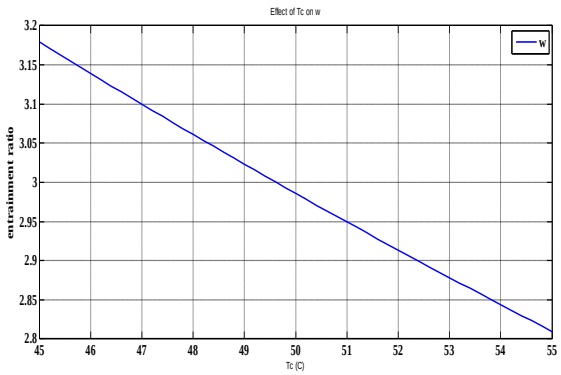

Fig. 8 Effect of Tc on entrainment ratio,ω

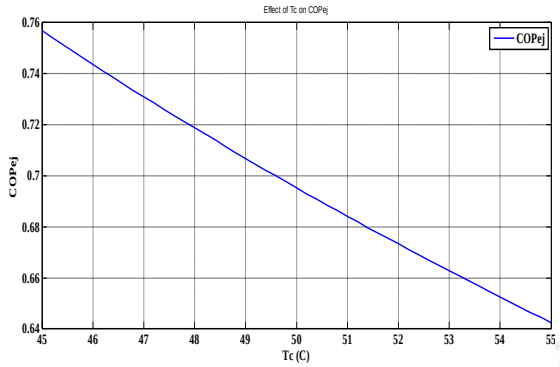

Fig. 9 Effect of Tc on COP of ejector cycle

4.3.3 Effect of T_e on COP of combined VCR-VER system

Figure 10 shows the effect of T_c on the COPs of combined VCR-VER systems. The COP decreases as the condensing temperature increases. The combined VCR-VER system is superior to the basic system in all cases.

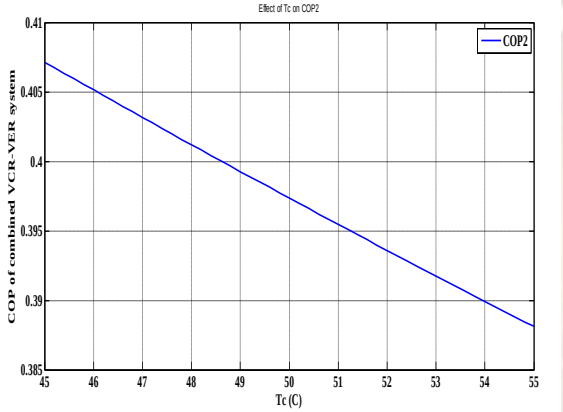

Fig. 10 Effect of Tc on COP of combined VCR-VER system, COP2

4.4 Effect of α_{PP}

The ejector performance is strongly affected by the primary flow pressure, P_{13}, the secondary flow pressure, P_7 and the back pressure, P_8. The back pressure, P8, was fixed, while the primary pressure, P_{13}, was changed to vary α_{PP}. The results in this section were obtained by varying α_{PP} from 2.0 to 2.5 at Tc = 50 °C, Te = -5 °C, α_A = 7.0 and α_{PS} = 1.5.

4.4.1 Effect of α_{PP} on cooling capacity

The effect of α_{PP} on the cooling capacity of system with R600a is shown in Figure 11. The results show that the cooling capacity of the combined VCR-VER system decreases slightly with α_{PP}. The secondary mass flow rate (i.e. the mass flow rate in the booster and the expansion valve B) decreases with increasing primary flow pressure. Therefore, the cooling capacity of the combined VCR-VER system decreases because the cooling capacity of the ejector cycle is decreased.

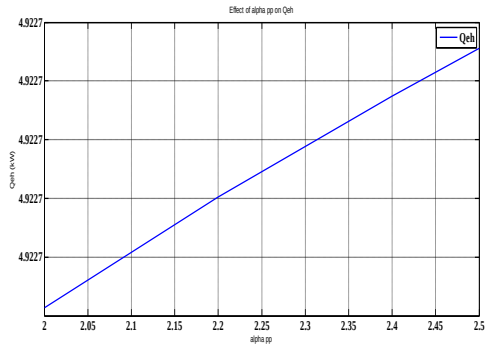

Fig.11 Effect of α_{PP} on cooling capacity, Qeh (kW)

4.4.2 Effect of α_{PP} on entrainment ratio

The performances of the basic system, the ejector cycle for various α_{PP} are shown in figure 13. The ejector performance characteristics indicate that the entrainment ratio is reduced as the primary flow pressure increases. In addition, as the primary flow pressure increases, the work input to the pump increases. As a result, COP_{ej} decreases as seen in Figure 13.

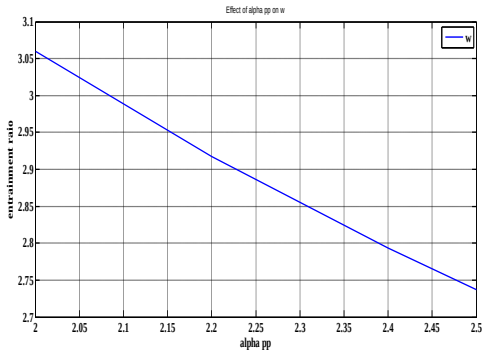

Fig.12 Effect of α_{PP} on entrainment ratio

4.4.3 Effect of α_{PP} on COP of combined VCR-VER system

The COP increase with the combined VCR-VER system is better at lower pressure ratios. As shown in figure 15. However, the pressure ratio is restricted by the critical pressure ratio of the ejector nozzle is,

$$\alpha_{pp,cr} = \left(\frac{2}{\kappa+1}\right)^{\frac{\kappa}{1-\kappa}}$$

where k is the gas specific heat ratio. The critical pressure ratios for R600a is about 1.70, which means that the pressure ratio should be larger than 1.70 to ensure that the ejector works normally.

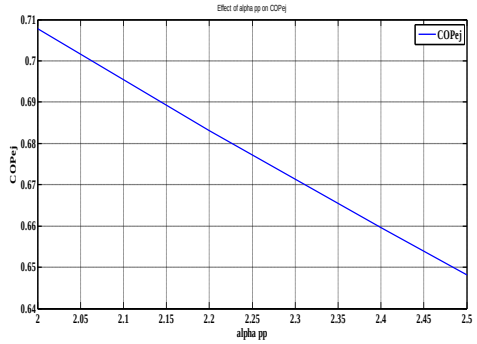

Fig.13 Effect of α_{PP} on COP of ejector cycel

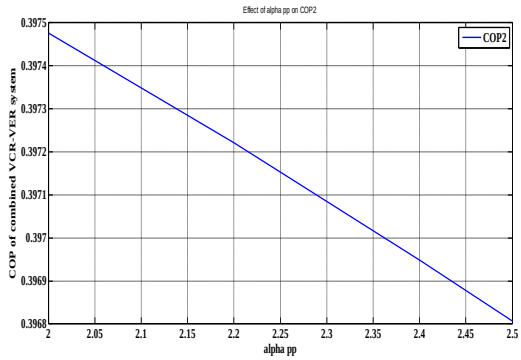

Fig.15 Effect of α_{PP} on COP of combined VCR-VER system, COP_2

4.5 Effect of α_A

4.5.1 Effect of α_A on cooling capacity

The influence of the area ratio, α_A, on the system performance was analyzed for T_c = 50 °C, T_e= -5 °C, α_{PP} = 2.1 and α_{PS} = 1.5. The ejector nozzle throat diameters D_t were determined by the heat balance in the generator. The ejector mixing chamber diameter was calculated by D_t and α_A.

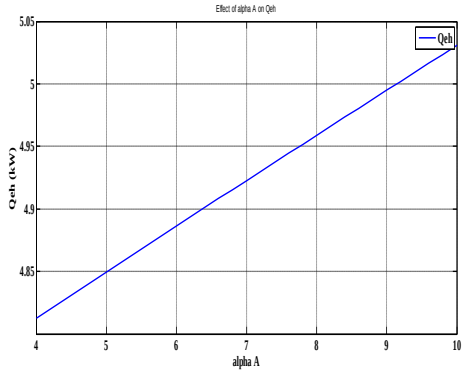

Fig.16 Effect of α_A on cooling capacity, Q_{eh} (kW)

Figure 16 shows the effect of α_A on the cooling capacity of both systems. The results show that the cooling capacity of the combined VCR-VER system increases with increasing α_A, while the cooling capacity of the basic system is not affected by the ejector geometry

4.5.2 Effect of α_A on entrainment ratio

The variation of the entrainment ratio and ejector cycle COP with α_A is shown in Fig. 17. The entrainment ratio and ejector COP increase greatly as α_A increases. The improved ejector performance directly improves the entire system performance.

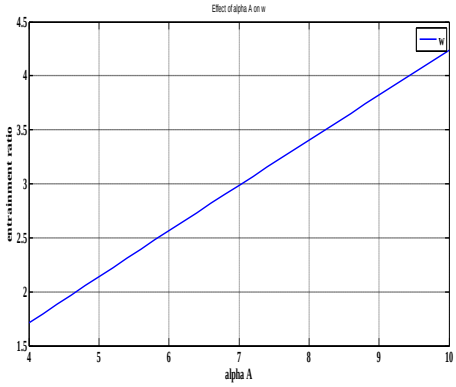

Fig.17 Effect of α_A on entrainment ratio

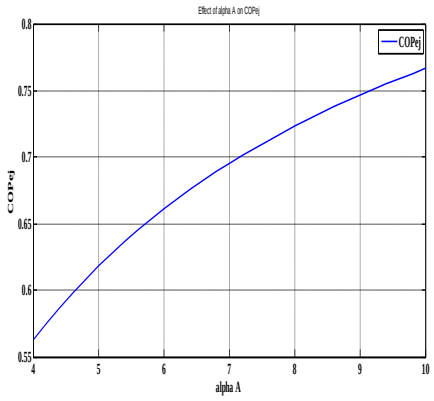

Fig.18 Effect of α_A on COP of ejector cycel

4.5.3 Effect of α_A on COP of combined VCR-VER system

The COP of the combined VCR-VER system increases with increasing area ratio as shown in Figure 17. The COP improvement with the combined VCR-VER system will be even higher with larger area ratios. However, larger area ratios require a higher-pressure ratio, α_{pp}, to drive the ejector (Huang et al., 1999). Thus, the area ratio needs to be carefully designed to optimize the system.

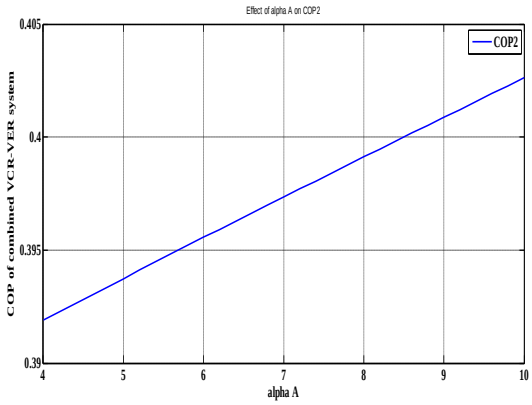

Fig.19 Effect of α_A on COP of combined VCR-VER system, COP_2

CONCLUDING REMARK

A combined VCR-VER refrigeration system was developed by combining a basic vapor compression refrigeration cycle with an ejector cooling cycle in parallel. The governing equations of each component were derived based on the energy and mass conservation laws. The system performance was analyzed as a function of five important variables. The results show that the combined VCR-VER system is superior to the basic refrigeration system over a wide range of operating conditions. The main results can be summarized as follows.

1. The combined VCR-VER refrigeration system with the parallel ejector cycle significantly improves the COP when the compressor discharge temperature is larger than 100 °C. Simulations give an average COP increase for the combined VCR-VER system with R600a is 3.086%.
2. As with the basic vapor compression refrigeration system, the COP of the combined VCR-VER system increases with the evaporating temperature and decreases with the condensing temperature.
3. The ejector is the key component of the combined VCR-VER refrigeration system. The ejector geometries and operating conditions greatly influence the ejector performance and the whole refrigeration system. A reduced primary flow inlet pressure or increased area ratio and secondary flow inlet pressure increases the COP of both the ejector cycle and the combined VCR-VER cycle. However, the two variables of primary flow inlet pressure and area ratio are contradictory since a high critical pressure ratio is required for a great area ratio to make the ejector operate in the critical mode. In practice, the pressure ratio and the ejector area ratio need to be carefully designed to optimize the combined VCR-VER system for the best COP.

REFERENCES:

1. Sun, D.W., Eames, W.I., Aphornratana, S., 1996. Evaluation of a novel combined ejector absorption refrigeration cycle, I computer simulation. Int. J. Refrigerat. 19, 8.
2. Sun, D.W., 1997. Solar powered combined ejector-vapour compression cycle for air conditioning and refrigeration. Energ. Convers. Manag. 38 (5), 479-491.
3. Arbel, A., Sokolov, M., 2004. Revisiting solar-powered ejector air conditioner e the greener the better. Sol. Energ. 77, 57-66.
4. Herna´ndez, J., Dorantes, R., Best, R., Estrada, C., 2004. The behaviour of a hybrid compressor and ejector refrigeration system with refrigerants 134a and 142b. Appl. Therm. Eng. 24.
5. Jaya, P.V., Prakasha, R., Srinivasa, M., 2005. Studies on an Ejector absorption Refrigeration Cycle With New Working Fluid Pairs. In World Climate and Energy Event, pp. 113-122.
6. Elakdhar, M., Nehdi, E., Kairouani, L., 2007. Analysis of a compression/ejection cycle for domestic refrigeration. Ind. Eng. Chem. Res. 46, 4639-4644.
7. Blitzar International., 2007. Available on October 2008, de IIFIIR: www.iifiir.org/en/doc/1029.pdf.
8. Petrenko, V.O., Huang, B.I., Ierin, V.O., 2011. Design theoretical study of cascade CO2 sub-critical mechanical compression/butane ejector cooling cycle. Int. J. Refrigerat 34, 1649-1656.
9. Yinhai Zhu, Peixue Jiang, 2012. Hybrid vapor compression refrigeration system with an integrated ejector cooling cycle. Int. J. of refrigeration 35,68-78
10. Abdulateef, J., Sopian, K., Alghoul, M.A., Sulaiman, M., 2009. Review on solar-driven ejector refrigeration technologies. Renew. Sustain. Energ. Rev. 13, 1338-1349.
11. Chunannond, K., Aphornratana, S., 2004. Ejectors: applications in refrigeration technology. Renew. Sustain. Energ. Rev. 8, 129-155.
12. Huang, B.J., Chang, J.M., Wang, C.P., Petrenko, V.A., 1999. A 1-D analysis of ejector performance. Int. J. Refrigeration 22, 354-364.
13. Zhu, Y.H., Cai, W.J., Wen, C.Y., Li, Y.Z., 2007. Shock circle model for ejector performance evaluation. EnergyConvers. Manage. 48, 2533e2541
14. Zhu, Y.H., Li, Y.Z., 2009. Novel ejector model for performance evaluation on both dry and wet vapors ejectors. Int. J. Refrigeration 32, 21-31.
15. Bartosiewicz, Y., Aidoun, Z., Desevaux, P., Mercadier, Y., 2005. Numerical and

experimental investigations on supersonic ejectors. Int. J. Heat Fluid Flow 26, 56e70.
16. Aphornratana, S., Chungpaibulpatana, S., Srikhirin, P., 2001. Experimental investigation of an ejector refrigerator: Effect of mixing chamber geometry on system performance. Int. J. Energy Rese. 25, 397-411.
17. Sun, D.W., 1997. Experimental investigation of the performance characteristics of a steam jet refrigeration system. Energy Sources 19, 349-367.